# A kinetic model of sugar metabolism in peach fruit reveals a functional hypothesis of markedly low fructose-to-glucose ratio phenotype

Elsa Desnoues, Michel Génard, Bénédicte Quilot-Turion, Valentina Baldazzi

Short title:
Kinetic model of sugar metabolism in peach fruit

Corresponding author:
Valentina Baldazzi
Valentina.Baldazzi@inra.fr
Tel: +33 (0)4 92 38 64 22

Title:
**A kinetic model of sugar metabolism in peach fruit reveals a functional hypothesis of markedly low fructose-to-glucose ratio phenotype**

Authors:
Elsa Desnoues[1,2], Michel Génard[1], Bénédicte Quilot-Turion[2], Valentina Baldazzi[1]
[1] UR1115, PSH, INRA, Avignon, France; [2] UR1052, GAFL, INRA, Montfavet, France;

Significance statement:
The use of experimental enzymatic kinetics and inclusion of cell compartment in the construction of a model of sugar metabolism makes it possible to identify a functional hypothesis for a marked low-fructose phenotype in peach fruit.

Author contributions:
VB, MG and BQ designed the study. ED, VB and MG built the model. ED performed the simulations. All authors analyzed the data and wrote the manuscript.

Funding information: This research was partially funded by grants from the ‘Environment and Agronomy’ division and the ‘Plant Biology and Breeding’ division (FructoPech and PhenoPech) of the Institut National de la Recherche Agronomique, France and by a grant from the PACA Region, France.

Corresponding author email: Valentina.Baldazzi@inra.fr

**A kinetic model of sugar metabolism in peach fruit reveals a functional hypothesis of markedly low fructose-to-glucose ratio phenotype**

**Abstract**:

The concentrations of sugars in fruit vary with fruit development, environment, and genotype. In general, there were weak correlations between the variations in sugar concentrations and the activities of enzymes directly related with the synthesis or degradation of sugars. This finding suggests that the relationships between enzyme activities and metabolites are often non-linear and are difficult to assess. To simulate the concentrations of sucrose, glucose, fructose and sorbitol during the development of peach fruits, a kinetic model of sugar metabolism was developed by taking advantage of recent profiling data. Cell compartmentation (cytosol and vacuole) was described explicitly, and data-driven enzyme activities were used to parameterize equations. The model correctly accounts for both annual and genotypic variations, which were observed in ten genotypes derived from an interspecific cross. They provided important information on mechanisms underlying the specification of phenotypic differences. In particular, the model supports the hypothesis that a difference in fructokinase affinity could be responsible for a low fructose-to-glucose ratio phenotype, which was observed in the studied population.

## INTRODUCTION

There is high variability in sugar concentrations of peach accessions (Cantín *et al.* 2009). Although sugar content varies immensely, the concentration of fructose and glucose is nearly equal in most commercial varieties of peach at maturity. In wild or ornamental peaches, fructose-to-glucose ratio is usually between 0 and 0.1 because fructose concentration is very low (Moriguchi *et al*. 1990; Kanayama *et al*. 2005). Hereafter, this particular phenotype will be referred to as 'low fructose-to-glucose ratio' phenotype. Because there is relative variation in the sweetness of sugars (Pangborn 1963), it is important to understand the mechanisms that control sugar metabolism. With this knowledge, varieties that meet consumers' expectations can be created.

In peach, carbon enters the fruit in the form of sucrose and sorbitol. These are two main end products of photosynthesis in source organs (Moriguchi *et al.* 1990). As shown in Figure 1, the arrows F1 and F2 schematically represent carbon flows in the cell. In cell wall, the enzyme invertase hydrolyzes a proportion of sucrose into glucose and fructose, which then

enters the cytoplasm of cells (F3). Sugars (sucrose, glucose, and fructose) and sugar alcohol (sorbitol) are mostly metabolized in cytosol, but they can be stored into vacuole via specific transporters (F4, F5, F6, F7, F8 and F19). In cytosol, fructose and glucose are produced by hydrolyzing sucrose (F9, F10, and F13) or cytosolic sorbitol (F11 and F12) (Moriguchi *et al.* 1990). In reactions catalyzed by fructokinase (FK) (F14) and hexokinase (HK) (F15), fructose and glucose are further phosphorylated (Kanayama *et al.* 2005). The resultant hexose phosphates are used for any of the following purposes: i) resynthesis of sucrose (F16), ii) synthesis of other compounds, mostly structural compounds (F17), and iii) respiration via citric acid cycle (F18).

In recent studies, it was found that a large number of metabolites and enzymes' maximal activity are involved in sugar metabolism during fruit development. These studies have proved that there is no clear link between the concentration of given sugars and enzymatic activity of related enzymes (Biais *et al.* 2014; Desnoues *et al.* 2014). This finding suggests that the regulation of sugar metabolism is complex, and it results from the interaction of several components in a system. Therefore, an integrative approach is needed to elucidate metabolic networks and the regulatory mechanisms of these networks responsible for phenotypic changes.

Several approaches have been undertaken to model metabolic networks in plants with different levels of complexity (Rios-Estepa & Lange 2007). Among possible approaches, kinetic models are very useful to either investigate functional hypotheses or to perform *in silico* experiments, which provide mechanistic descriptions of metabolic functions. Kinetic modeling has been successfully applied to several metabolic networks in plants (Uys *et al.* 2007; Curien *et al.* 2009; Nägele *et al.* 2010; Nägele & Weckwerth 2014). Beauvoit *et al.* (2014) recently developed a kinetic model for tomato fruits. The model simulates sugar metabolism of tomato fruit and its reprogramming according to various stages of development. For peach, Génard & Souty (1996) developed a model that simulated the accumulation of sugar during the development of fruits. This model was used to explore natural phenotypic diversity of peach fruits. In particular, special attention was given to observed differences in fructose-to-glucose ratio (Wu *et al.* 2012). Despite having a satisfactory agreement with experimental data, the structure of the model proposed by Génard and Souty (1996) was too simple and gave little evidence to support a hypothesis that explains low fructose concentration. One of the major limitations of this model was that it did not account for cell compartmentation. Subcellular compartmentation is essential for sugar accumulation (Patrick *et al.* 2013; Génard *et al.* 2014), and it can significantly affect

metabolite concentrations (Sweetlove & Fernie 2013, Fettke & Fernie 2015, Beauvoit *et al.* 2014).

The objective of present study is to decipher the mechanisms of sugar accumulation during peach fruit development.. Based on this objective, a new kinetic model of sugar metabolism was developed. This model provided an explicit representation of cellular compartmentation (cytosol and vacuole) and data-driven enzymatic activities. The model is able to simulate the accumulation of sugars (sucrose, glucose, and fructose) and sugar alcohol (sorbitol) on the timescale of peach fruit development, which extends from stone hardening to maturity. It correctly accounts for both genetic and annual variations, which were observed in the experimental data of ten genotypes. The implementation of enzyme kinetic parameters in equations allows a direct identification of molecular mechanisms, which are involved in specific phenotypic differences during fruit development.

## RESULTS

### A dynamical model of sugar metabolic network in peach

A dynamic model was built to determine sugar metabolism in the mesocarp of peach fruit as shown in Figure1. The model describes carbon flows through different metabolites and cell compartments during fruit growth, which form a set of ordinary differential equations (Eqn S1). Metabolic network represented by the model is similar to those described by Moriguchi *et al.* (1990), Etienne *et al.* (2002), and Kanayama *et al.* (2005). Hexose phosphates (glucose-1-phosphate, glucose-6-phosphate, fructose-6-phosphate, and UDP-glucose) were represented as a single pool, because kinetic information on their mutual interconversion was lacking. Enzymatic reactions were represented by an irreversible Michaelis–Menten (MM) equation. Only allosteric regulation of AI was taken into account based on a principle of parsimony (see Model description in ‘Experimental procedure’ section).

Based on the results of cytological analyses, cytosol and vacuole were compartmentalized explicitly (see Experimental Procedure). Figure S1 shows experimental data and fitted curves, which illustrate the variation in vacuole-to-cell ratio and cytosol-to-cell ratio with the development of peach fruit. These cytological data completely agree with the data of peach leaves in a study conducted by Nadwodnik & Lohaus (2008). These proportions were used in the model to split fruit fresh weight into vacuole and cytosol fresh weights and to calculate appropriate metabolite concentrations, which governed enzymatic reactions within both compartments. In contrast to cytosol and vacuole, the apoplastic compartment was not

explicitly represented in the model but the effect of cell wall invertase was taken into account by partitioning sucrose supply coming from the plant into hexose supply (F3) according to a time-dependent fraction $\lambda_{Suc}(t)$ (see Model description in 'Experimental procedure' section).

During fruit development, different mechanisms are used for exchanges between cytosol and vacuole in specific metabolites. Several active and passive transporters specific to sugars have been described at tonoplast surface of plant cells (Doidy *et al.* 2012; Martinoia *et al.* 2012; Ludewig & Flügge 2013). They are included into the model according to available literature data (see 'Experimental procedure' section)

The developed model was calibrated for ten genotypes by estimating 14 parameters (see Experimental Procedure, Table S1). During peach fruit development, the evolution in the concentration of four sugars (sucrose, glucose, fructose, and sorbitol) was accurately simulated. It correctly reproduced genetic diversity, which was observed within the genotypes included in this study (Figure 2a, Table S2). This includes a particular phenotype with a low fructose-to-glucose ratio. In addition, two of the ten genotypes (one for each fructose type) were studied for two years (Figure 2b). In this case, the model was able to accurately predict the evolution of sugar concentration in both years by estimating a single set of parameters per genotype.

**Flow distribution through metabolic network**

For each genotype and their evolution during fruit development, the model enabled the calculation of intermediate carbon flows across the entire pathway. Figure S2 displays predicted temporal evolution of the system's flows, which were expressed as a percentage of the total carbon uptake. The ten genotypes had a similar flow distribution through the metabolic network. At the beginning of fruit development, sorbitol supply (F2) and hexose supply (F3) (fructose and glucose) represented main sources of carbon for peach fruit. This accounted for almost half of the total C flow because of the activity of cell-wall invertase. With the development of peach fruit, the activity of cell-wall invertase decreased and the concentration of sucrose (F1) increased (35% on average at maturity). A large concentration of sucrose was stored in the vacuole as the flux of F4 increased with sucrose supply in the cell. Only a minor fraction was used for cell metabolism and hexose synthesis in the cytosol. However, flow catalyzed by acid invertase (F13) in the vacuole, increased at maturity due to increasing concentration of vacuolar sucrose. In the cytosol, cell metabolism was mostly fueled by sorbitol. Although sorbitol represented 35% of sap sugar (Figure S3), it had a low

concentration in peach fruit. This results from its high degradation rate in cytosol, which provided carbon for respiration (F18), structural compounds (F17) and other molecules for synthesis (SDH F11 and SO F12), and low storage in vacuole (F19).

Net flows of tonoplastic hexose transport (F5-F6 and F7-F8) varied during fruit development. Early stages were characterized by hexose storage in vacuole, but the flow was reversed near the intermediate stage of fruit development. The flow catalyzed by AI (F13) was higher at peach fruit maturity. Fructose and glucose were produced in vacuole and contributed to the synthesis of structural components (F17) and respiration (F18) by degrading cytosol (FK F14 and HK F15).

Flows catalyzed by enzymes SuSy (F9), SDH (F11), and SO (F12) displayed reduced variation during fruit development across ten genotypes, except for genotype C227, which had a higher F9 flow for two simulated years. Larger genetic variability was found for flows involved in the reaction of NI (F10), AI (F13), FK (F14), and HK (F15) and the re-synthesis of sucrose by SPS and SPP (F16).

**Sugar compartmentation**

The distribution of sugars within the vacuole and cytosol were explored with model compartmentation. The model predicted a very low concentration of sucrose in cytosol (Figure S4), indicating that sucrose entering the fruit or synthesized via hexose phosphate was transported into the vacuole or directly metabolized. This is compliant with the increase in sucrose import flow (F4) and the light flow of sucrose degradation in cytosol (SuSy F9 and NI F10) (Figure S2). In contrast, remaining three sugars had similar concentrations in both the compartments (Figure S4). The action of passive transport (it depends on concentration gradient) contributed largely to this feature.

**Origin of the observed phenotypic variability**

To investigate the link between parameters and phenotypes, a PCA analysis was performed on parameter values estimated for all genotypes. Inter-genotype variability of parameter values was higher than intra-genotype variability. The PC1-PC2 plan represents 42.8% of the variation observed in dataset (Figure S5), but it does not allow the separation of two fructose-to-glucose phenotypes. Indeed, it contrasts genotypes according to other characteristics, that is, the direction of hexose transport between cytosol and vacuole (F5 and F7 was driven by VmTactiGlu and VmTactifFru, respectively) and according to the proportion of sucrose hydrolyzed upon its entry into the cell (F1 and F3 was modified by

λSuc). The genotypes C216 and C227 were further separated according to the synthesis of hexose phosphates by Khk and their following use for the synthesis of new compounds (F17 flow was driven by OthComp).

Figure 3a shows that the two fructose-to-glucose phenotypes could be better separated by third principal component. The separation between two phenotypes seems to be mostly due to a difference in the estimation of parameters Kfk, TpassifSor, λSuc, and Khk to a lesser extent (Figure 3b). Among these parameters, only the parameter Kfk is directly linked with fructose metabolism (degradation enzyme). For the 'low-fructose-to-glucose ratio' group, the significantly lower $K_M$ value of FK indeed resulted in increased fructose degradation (Figure S6). Other parameters (TpassifSor, λSuc, Khk and TactifSuc) may point to an indirect effect via a change in substrate concentration.

Parameters directly linked to enzymes involved in fructose synthesis (Ksusy) and storage (TpassifFru), were not detected through PCA analysis. In case of 'low-fructose-to-glucose ratio' group, TpassifFru displayed slightly larger values and it was associated with observed phenotype; however, the difference was not significant (Figure S6). TpassifFru parameter enables the exchange of fructose between vacuole and cytosol, according to concentration gradient. In our model, TpassifFru only acts as an exporter due to the presence of an active transporter that stores fructose in the vacuole. The slightly higher values of TpassifFru may contribute to reduce fructose storage in the vacuole, allowing a higher degradation of fructose in cytosol.

**Functional hypotheses for the 'low fructose-to-glucose ratio' phenotype**

To explore functional hypotheses of 'low fructose-to-glucose ratio' phenotype, we simulated concentrations of sugars and sequentially exchanged the value of each parameter with the average estimated value of opposite fructose type. For the genotypes with 'standard fructose-to-glucose-ratio' phenotype, fructose concentration was not affected by modifying parameters with the average estimated value of low-fructose genotypes. The change of the parameter TpassifFru induced a partial decrease in fructose concentration (Figure S7) but only the modification of Kfk parameter was able to decrease fructose concentration almost to zero, as observed in low 'fructose genotypes' (Figure 4a). The same approach was applied to genotypes with 'low fructose-to-glucose ratio' phenotype, and parameter values were estimated from genotypes with standard phenotype. Only simulations involving a modification of Kfk parameter resulted in higher fructose concentrations (Figure 4b), which

was comparable to what was observed in standard genotypes. In all cases, the modification of Kfk did not alter concentrations of other sugars.

Based on these simulations, the affinity of FK is a good candidate that explains the 'low fructose-to-glucose ratio' phenotype. To further explore mechanisms involved in fructose degradation, the consequences of modified Kfk were examined on system's flows (Figure 5). As expected from the high connectivity of the network, results indicate that modified fructokinase affinity affected most metabolic fluxes and induced a reorganization of the whole-system level. When Kfk was lowered to the average value estimated in 'low-fructose' genotypes, fruit metabolism was activated in standard genotypes. Indeed, sucrose degradation (F9, F10, and F13), its storage in vacuole (F4), hexose degradation into hexose-P (F14 and F15), sucrose re-synthesis (F16), and hexose transport were increased between vacuole and cytosol (F7-F8 and F5-F6). Conversely, when mean Kfk value of genotypes with the 'standard fructose-to-glucose-ratio' phenotype was used for the simulation of genotypes with 'low fructose-to-glucose ratio' phenotype, sucrose degradation, transport, and re-synthesis were reduced. Among the most affected metabolic fluxes, sucrose degradation by AI (F13) changed by 10% to 38% following the modification of Kfk and depended on the genotype (Figure S8 and Table S3). Moreover, the variation of tonoplastic transport of fructose (F7-F8) exceeded 30%. The latter effect is not surprising because this flow depends directly on the gradient of fructose concentration across tonoplast membrane.

**A virtual classification experiment supports the role of Kfk as determinant for the 'low fructose-to-glucose ratio' phenotype**

Previous section explored the effect of different fructokinase affinity on genotypes included in this study, suggesting an important role in the emergence of a 'low fructose-to-glucose ratio' phenotype. Given the small panel of genotypes included in this study, other mechanisms might be involved and encoded in specific combinations of parameters. To ensure that Kfk 'alone' has an effective role in 'low fructose-to-glucose ratio' phenotype, an *in silico* classification experiment was performed. This experiment was based on the generation of a large number of virtual genotypes, which contrasted Kfk values. To achieve this objective, 100,000 virtual genotypes were first simulated and values of all parameters were taken randomly within the range of the previous estimations (see Experimental procedure). The highest correlation of final fructose-to-glucose ratio was obtained with Kfk parameter (Pearson correlation 0.57, *P-value* < 0.001). This confirmed that fructokinase affinity was involved in maintaining the balance between fructose and glucose content (Figure

S9). Hence, a new set of simulations was conducted. For half of the simulations, Kfk value was fixed at an average estimated value of 'standard fructose-to-glucose-ratio' phenotype (i.e. 16.58 mg.gFW-1). For the remaining simulations, Kfk value was fixed at an average estimated value of 'low fructose-to-glucose ratio' phenotype (i.e. 1.52 mg.gFW-1). Figure 6 shows the resultant fructose-to-glucose ratio at maturity. A significantly lower ratio was observed for the simulations of with Kfk value from 'low fructose-to-glucose ratio' phenotype (Wilcoxon test, *P-value* < 2.2e-16) than those with Kfk value from 'standard fructose-to-glucose ratio' phenotype. The distribution of possible phenotypes was remarkably narrow with a low Kfk value: a high fructokinase affinity (low $K_M$ value) seems to guarantee a low fructose concentration (i.e fructose-to-glucose ratio below 0.2), which is almost independent of other parameters' values. On the other hand, a large phenotypic variability was observed within simulations with high Kfk value (these were associated with 'standard fructose-to-glucose ratio' phenotype) as well as emerging correlations with other model parameters, such as Khk and parameters linked to tonoplastic transport (Figure S9). This suggests that other mechanisms may participate with fine fructose-glucose balance in standard genotypes.

## DISCUSSION

We developed a dynamic model of sugar metabolism which was able to simulate the accumulation of sucrose, glucose, fructose, and sorbitol during peach fruit development. In this model, enzymatic activities were combined with subcellular compartmentation (cytosol and vacuole) and their evolution over time. When applied to ten genotypes with different fructose phenotypes, the model correctly accounted for both genetic and annual variations observed in experimental data. Because of its mechanistic nature, the model is a valuable tool to investigate the mechanisms involved in the accumulation of sugars in peach fruit.

### Model estimation of $K_M$ values

Previous studies have shown the presence of different isoforms of FK, SuSy, and HK enzymes in peach fruits, which have different affinity for their substrate (Schaffer and Petreikov 1997; Kanayama *et al.* 1998; Tanase and Yamaki 2000; Kanayama *et al.* 2005). $K_M$ values related to these enzymes were estimated in this study. However, the estimated $K_M$ values were higher than expected. Previous studies (Kanayama *et al.* 1998; Kanayama *et al.* 2005) have reported that FK enzymes contained two isoforms whose affinity for fructose was equal to 1.3 mM and 0.054 mM. In the present model, the average affinity was estimated to be 100 mM and 5.5 mM depending on the fructose type (18 and 1 mg g $FW^{-1}$; Figure S6). For

SuSy, the average estimated affinity for sucrose was 300 mM (140–150 mg g $FW^{-1}$; Figure S6), whereas a $K_M$ of only 4.8 mM was observed in peach fruit (Moriguchi & Yamaki 1988).

Many reasons account for the overestimation of $K_M$ values. In our model, fructokinase and hexokinase are supposed to act on fructose and glucose substrate, respectively. Thus, hexokinase and fructokinase enzymes were considered as abstracts of real enzymes *in vitro*, referring to total glucose and fructose phosphorylating activity, respectively, rather than specific enzyme species. This partially explains the discrepancies between estimated and measured in vitro $K_M$ values.

A second source of overestimation of $K_M$ values is as follows: following our model selection procedure (see 'Model description' section), the mechanisms of enzyme inhibition were not represented for aforementioned enzymes. (Morell & Copeland 1985; Doehlert 1987; Ross & Davies 1992; Schaffer & Petreikov 1997). In the absence of an explicit description of enzyme inhibition, the estimated $K_M$ values were interpreted as an effective average of enzyme affinity that depends on specific physiological conditions or genotypes included in this study.

**Sorbitol: the driver of sugar metabolism in peach**

Sugar metabolic network is well known in model species, such as tomato and *Arabidopsis thaliana*, because it plays important role in carbon and energy metabolism and signaling; however, it may differ among species. Peach, as well as most of Rosaceae, differs from model species in that an alcohol sugar, sorbitol, is translocated from source to sink organs by providing an additional metabolic pathway, which is not well described.

The model points to a different utilization of sucrose and sorbitol from sap, providing clues to the role of sorbitol metabolism in peach. Almost all sucrose that is not hydrolyzed into apoplasm, is stored in vacuoles. Sorbitol is highly degraded in cytosol, and it is the main driver for the synthesis of structural compounds and respiration. The high sorbitol degradation results in the low concentration observed in peach fruit, which may be an adaptation for the reduction of cytosolic sorbitol that can be toxic and cause tissue necrosis (Sheveleva *et al.* 1998).

In a previous study, the re-synthesis of sorbitol through sorbitol-6-P-dehydrogenase was demonstrated in pear (Yamaki & Moriguchi 1989) and loquat (Abnasan *et al.* 1999) fruits, but the same synthesis reaction may not be suitable for peach fruit (Sun *et al.* 2011). The results from the model supported this conclusion. This indicates that sorbitol re-synthesis was not necessary for a good fit of sorbitol concentration in all genotypes of this study.

**Vacuolar transport and sugar repartition within the cell compartments**

In this study, dynamic model accounted for cellular compartmentation and explicit representation of vacuole and cytosol. Cellular compartmentation is essential for high-level sugar accumulation (Patrick *et al.* 2013) and unbiased metabolomic analysis. The activities or concentration patterns can change substantially when expressed in terms of total cell mass or individual subcellular compartments (Génard *et al.* 2014). Beauvoit *et al.* (2014) showed this effect on the concentrations of ATP and ADP, which diminished over time when expressed in a global manner but remained constant when expressed with respect to cytosol volume.

The model therefore provides an insight into the distribution of sugars in vacuole and cytosol. It is difficult to obtain this information experimentally. The model predicts that fructose, glucose, and sorbitol have almost the same concentration in both compartments. In contrast, the concentration of sucrose was much higher in vacuoles than in cytosol. Very few studies reported about the concentration of sugar within cellular compartments. Farré *et al.* (2001) experimentally determined the concentrations of sugars in cytosol and vacuole in potato tuber. Beauvoit *et al.* (2014) explored this feature via a metabolic model in tomato fruit. These two studies were in agreement with the present model, which states that the main sugar of a given fruit has high concentration in the vacuole, but it is almost absent from cytosol. In other sugars, an equivalent concentration is present between two compartments.

This feature is harder to assess while comparing sugar repartition, which is based on quantity. This is because of the uncertainty in volumes of compartments. Considering the relative compartment volumes of vacuole and cytosol in potato tuber cells, Farré *et al.* (2001) reported that 85% of sugar had to be in vacuoles as it had an equal concentration in both compartments. Our model predicted a higher ratio of 90 to 95%, which can be explained by the differences in cytosol and vacuole volume in peach fruit with respect to potato tuber (Farré *et al.* 2001). These repartitions of sugars were also in agreement with those reported in apple fruit by Yamaki & Ino (1992). They estimated that the proportion of vacuolar sugar was between 81 and 88%. For peach fruit at maturity Jiang *et al.* (2013) reported that only 50 to 60% of sucrose, glucose, fructose, and sorbitol were present in vacuole. However, they did not give any indication of volumes of compartments in their study, impeding a comparison and further prediction of repercussions of low vacuolar sugar contents in terms of differences between cytosolic and vacuolar concentrations.

**Differences in FK affinity as a candidate mechanism for the 'low fructose-to-glucose ratio' phenotype**

Our model was applied to a panel of genotypes with different phenotypic traits, which paves the way to an in-depth investigation of molecular mechanisms underlying trait variations.

*In silico* experiments revealed that the fructose content was reduced by decreasing $K_M$ for FK. This was regardless of initial fructose concentration and independent of other parameter values. Similarly, a larger $K_M$ of FK increased fructose concentration of genotypes with 'low fructose-to-glucose ratio' phenotype. Such a result could not be achieved by modifying any other parameter. Therefore, FK is a good candidate for controlling 'low fructose-to-glucose ratio' phenotype. In addition, two isoforms of FK with a different affinity for fructose have been identified in peach (Kanayama *et al.* 1998; Kanayama *et al.* 2005). These isoforms may be in different proportions in two fructose types, which may result in differential degradation of fructose and emergence of two phenotypes.

In Arabidopsis leaves, a similar phenotype has been attributed to the action of tonoplastic transporter AtSWEET17; it is an exporter of fructose from vacuole to cytosol (Chardon *et al.* 2013). Similarly, Wei *et al.* (2014) found that the expression of MdSWEET4.1 transporter (phylogenetically similar to AtSWEET17) was higher in the leaves than in fruit of apples trees and that fructose concentration was lower in the leaves. The AtSWEET17 transporter is a bidirectional passive transporter (Guo *et al.* 2014), and its activity corresponds with TpassifFru parameter of the model. Model simulations showed that an increase in fructose export from the vacuole led to a decrease in fructose concentration in genotypes with the 'standard fructose-to-glucose-ratio' phenotype. However, the predicted decrease was less than the one obtained by reducing FK affinity parameter. On the other hand, TpassifFru is represented in the model as a passive transporter; its action only depends on fructose gradient across tonoplastic membrane. Its effect should thus be strengthened by coupling it with a "pump" mechanism, such as FK, which hydrolyzes fructose in cytosol. The fructose vacuolar transport and the two isoforms of FK are therefore compatible mechanisms that might act together for elaborating 'low fructose-to-glucose ratio' phenotype.

The model presented in this study proved to be a helpful tool for the investigation of sugar metabolism in peach and for the identification of mechanisms underlying phenotypic variability. Indeed, this study reveals that a difference in fructokinase affinity is associated with 'low fructose-to-glucose ratio' phenotype, which is observed in the studied population. Other mechanisms, such as a modification of fructose storage in vacuole, may participate and act with fructokinase affinity to cause this particular phenotype. Moreover, estimation of genetic parameters (parameters depending on genotypes) opens the way to further studies to

explore genetic control of sugar metabolism and to develop predictive tools. By estimating the parameter values of a large number of genotypes, it would be possible to identify genomic regions linked to parameter variations (QTL, quantitative trait loci). By integrating QTL information with model parameters, sugar composition in fruit could be simulated with genotypes of new allelic combinations (Reymond *et al.* 2004; Quilot *et al.* 2005; Quilot *et al.* 2016).

## EXPERIMENTAL PROCEDURES

### Plant material

Peach genotypes considered in this work were previously characterized by Quilot *et al*. (2004a). enotypes come from a progeny obtained from the following two back crosses: *Prunus davidiana* (Carr.) P1908 and *Prunus persica* (L.) Batsch 'Summergrand' and 'Zephyr'. Trees were 14 years old in 2012. They were planted in 2001 in a completely randomized design in the orchard of INRA Research Centre of Avignon (southern France). All genotypes were grafted on GF305 seedling rootstock. They were grown under normal irrigation, fertilization, and pest control conditions. All trees were homogeneously pruned and thinned. This study was performed on eight different genotypes, which were harvested in 2012. Two other genotypes were harvested in 2010 and 2011. Genotypes were selected to provide sufficient fruits for this experiment and to encompass population variability, which was based on data from previous years at maturity. Five genotypes of peach had 'standard fructose-to-glucose ratio'. The balanced fructose-to-glucose ratio at maturity was in the range 0.6–0.9, which corresponds with the ratio found in commercial varieties. Five genotypes had a 'low fructose-to-glucose ratio' because the proportion of fructose was lower than that of glucose (sugar composition was measured at maturity) (fructose-to-glucose ratio was in the range 0–0.08).

### Sugar concentration

For each genotype, the maturity date was extrapolated from previous data. Maturity level of fruits was defined as follows: i) fruits were no longer growing, ii) fruits were soft in texture, and iii) fruits could be picked easily. The expected interval between bloom and maturity dates was divided into six equal periods. Nine fruits were collected at each of the six sampling dates, and they were organized in three pools, with each pool containing three fruits. Thus, three biological replicates were obtained. All fruits were weighed and peeled: mesocarp was cut into small pieces, which were immediately frozen in liquid nitrogen and stored at –80

°C. The samples were then ground into a fine powder with liquid nitrogen and stored at –80 °C for future analyses. The concentrations of sucrose, glucose, fructose, and sorbitol were determined according to a procedure described by Desnoues *et al.* (2014).

**Fresh and dry weights of flesh**

Fruit fresh weight was determined at each sampling date for all genotypes. An estimation of stone fresh weight was performed to assess flesh fresh weight. Data was collected for several genotypes of the population from 2001 to 2008. As shown in Equation 1 (Eqn 1), this data was used to establish an empirical relationship between stone fresh weight (StoneFW) and fruit fresh weight (FruitFW).

$$StoneFW = a * \left(1 - \exp\left(-k * FruitFW\right)\right) \qquad \text{Eqn 1}$$

The parameters a and k were estimated using least squares method. This method was implemented with nls function in R software (R development Core Team 2006) for C216 (a = 6.05, k = 0.11), C227 (a = 12.13, k = 0.07), and eight other genotypes (a = 8.6, k = 0.06).

Flesh dry matter content was measured independently for all genotypes and at all developmental stages from. Flesh fresh weight powder (1 g) was dried for one week in an incubator at 37 °C and then weighed. Flesh dry weight was calculated from corresponding flesh fresh weight and flesh dry matter. Flesh fresh weight and flesh dry weights were then fitted with the curve described by Génard *et al.* (1991) (Eqn 2). This curve was fitted independently for each genotype, with W representing weight and t representing time:

$$W = W0 + p1 * \left(1 - \exp\left(-p2 * (t)\right)\right) + \frac{p3}{1 + \exp\left(-p4 * (t - p5)\right)} \qquad \text{Eqn 2}$$

The time courses of flesh fresh weight and dry weight are presented in Figure 7.

The individual dry weight was used for calculating respiration and sugar supply (see below). Fresh weight was used for converting sugar quantity (simulated by the model) into sugar concentration for the whole fruit or for cytosol and vacuole compartments.

**Cytological analysis**

To determine the evolution of cytosol-to-cell and vacuole-to-cell ratio during peach fruit development, a cytological analysis was performed on cells obtained from fruit flesh. Three fruits of C227 were collected at 57, 71, 92, and 120 days after bloom (DAB). Small flesh fragments were sampled on equatorial and perpendicular planes. Flesh fragments were fixed in glutaraldehyde and embedded in Epon 812, as described in a procedure by Beauvoit et al. (2014). Fifteen cells were measured for each orientation (equatorial and perpendicular

planes), fruit, and sample date. The width and height of vacuole and cell were measured with ImageJ software. The cell and vacuole were assumed to be spherical because there was no significant difference between the width and height for each orientation or between two orientations. The surface of the cell section, which was not occupied by the vacuole, was equally distributed between cell wall and cytosol (they were measured on ten cells at 57 and 120 DAB). Cell compartments were considered as a series of concentric spheres. Thus, the radius corresponding to cytosol and vacuole was determined. The volumes corresponding to vacuole, cytosol plus vacuole, and cell were calculated from their respective radii.

Within the cell, the proportions of vacuole and cytosol volume were determined at four different developmental stages for one genotype on three fruits per time point. A Fermi function was fitted with the experimental data (Figure S1).

**Measurement of sap sugar composition**

An exudation experiment was performed to determine the composition of phloem sap. The exudate of phloem sap was collected from cut apex of 21 young plants, which were obtained from selfing of a C216 genotype ('low fructose-to-glucose-ratio'). Plants were genotyped with markers surrounding QTL, which was responsible for 'low fructose-to-glucose-ratio' phenotype (Quilot *et al.* 2004b). Seven plants with homozygous *P. davidiana* allele at the locus, seven plants with homozygous *P. persica* allele, and seven plants heterozygous at specific locus were studied. The protocol was adapted from King and Zeevaart (1974). The apexes were cut in 20 mM EDTA solution at pH 7, and they were placed in 1 mL of 20 mM EDTA solution at pH 7 for 4 h in a dark box with saturated humidity. Two apexes of each genotype were used as negative controls, and they were placed in 40 mM $CaCl_2$ solution to limit phloem exudation. Exudation solution was frozen in liquid nitrogen and stored at –20 °C. Sucrose and sorbitol concentrations were determined by high-performance liquid chromatography (HPLC). Sap sugar composition was fairly constant among all assayed genotypes (Figure S3).

**MODEL DESCRIPTION**

The model describes carbon flows inside a peach fruit during fruit development, right from stone hardening to harvest, as a set of ordinary differential equations (Eqn S1).

For simplicity, the fruit was assumed to behave as a single big cell with two intracellular compartments, namely cytosol and vacuole. Carbon enters the fruit from the plant sap. Here it

is transformed by a complex cellular network, including enzymatic reactions and transport mechanisms between cytosol and vacuole. Measured fruit mass and external temperatures are included in the model.

*Enzymatic reactions*

When not considered explicitly, enzymatic reactions are described with an irreversible Michaelis-Menten (MM) kinetics in physiological direction (Eqn 3)

$$v = \frac{V_{max}[S]}{[S] + K_M} \qquad \text{Eqn 3}$$

Herein, [S] is substrate concentration in the considered cell compartment; $V_{max}$ is enzymatic activity and $K_M$ is Michaelis-Menten constant, describing enzymatic affinity towards substrate S. Allosteric regulations have been considered only when necessary (see section 'Model Selection procedure'). Only the allosteric regulation of acid invertase (AI) was retained and described as a competitive inhibition (Eqn 4)

$$v = \frac{V_{max}[S]}{K_M\left(1 + \frac{[I]}{K_I}\right) + [S]} \qquad \text{Eqn 4}$$

herein, [I] is inhibitor concentration (the sum of fructose and glucose concentration, as in the case of AI) and $K_I$ is inhibitor constant.

*Tonoplastic Transport*

In specific metabolites, cytosol and vacuole were exchanged following two mechanisms: active or passive transport.

*Active transport* was mediated by specific proteins carriers (antiporters), allowing sugar storage in vacuoles against concentration gradient. As for enzyme kinetics, this kind of transport was represented by an irreversible Michaelis-Menten equation (Boorer *et al.* 1996; Rohwer & Botha 2001; Borstlap & Schuurmans 2004) (Eqn 5).

$$v_{active} = \frac{VmTact[M_{cyt}]}{KmTact + [M_{cyt}]} \qquad \text{Eqn 5}$$

Here $[M_{cyt}]$ is cytosolic concentration of metabolite that is transported into vacuole; VmTact and KmTact represent maximal activity and MM constant of the carrier, respectively.

Few studies have investigated the concentration and evolution of transporters during fruit development. Beauvoit *et al.* (2014) showed that the activity of transporters increases with increasing age of tomatoes. It was assumed that the density of transporters per unit surface was constant. Consequently, transport increased proportionally with tonoplast surface during fruit development. Equation 6 (Eqn 6) is used for calculating total active transport flux:

$$Activetransport = \frac{VmTact}{KmTact + [M_{cyt}]} * [M_{cyt}] * Tsurf \qquad \text{Eqn 6}$$

where

$$Tsurf = (4 * pi)^{1/3} * (3 * gVac)^{2/3} \qquad \text{Eqn 7}$$

Equation 7 (Eqn 7) is used to determine the surface of vacuole (it is assumed to be spherical in shape), which is computed from vacuole's fresh weight gVac.

*Passive transport* facilitates the efflux of molecules, following their concentration gradient with respect to specific protein channels. Given its passive nature, this mode of transport can be represented by simple linear functions of the gradient concentration. As in the case of active carriers, it was assumed that the density of protein channels per unit surface remained constant. During fruit development, passive transport increased proportionally with respect to tonoplastic surface, Tsurf (Eqn 8):

$$Passivetransport = Tpassi * ([M_{cyt}] - [M_{vac}]) * Tsurf \qquad \text{Eqn 8}$$

Depending on sugar, different transport mechanisms have been reported in literature. In the case of sucrose, active sucrose transport occurred from vacuoles to cytosol; moreover, passive sucrose transport was never been demonstrated in a sink organ. Only an active import flow of sucrose into vacuole was represented in the model. Preisser & Komor (1991) reported that transporter saturation did not occur at physiological concentration of sugarcane. Therefore, we decided to represent this transport with a simple linear function of cytosolic sucrose concentration instead of an MM equation (F4). For hexoses, it was reported that both active and passive transports occurred in the vacuolar membrane of fruit (Martinoia *et al.* 2012). They were therefore included in the model (F5, F6, F7, and F8). Hexose active transporters were represented with an MM equation with a competition between fructose and glucose as

done in Beauvoit *et al.* (2014). Very little information is available on sorbitol transporters, and none of this information pertains to tonoplast (Wei *et al.* 2014). However, a tonoplastic transport mechanism is at least required to transport sorbitol in vacuoles of peach, so sorbitol transporter was considered as passive transport (F19) (Jiang *et al*. 2013).

**Respiration**

Fruit respiration was calculated as the sum of both maintenance respiration and growth respiration, according to growth-maintenance paradigm (Cannell and Thornley, 2000) (Eqn 9):

$$\frac{dCresp}{dt} = q_m DW\, Q_{10}^{\frac{(T-20)}{10}} + q_g \frac{dDW}{dt} \quad \text{Eqn 9}$$

Here, DW is the fruit dry mass; $q_g$ is the growth respiration coefficient; $q_m$ is the maintenance respiration coefficient at 20 °C; $Q_{10}$ is the temperature ratio of maintenance respiration; and T is temperature (°C).

Respiration did not exhibit any significant difference between genotypes (Desnoues et al. 2014). To simulate the respiration of all genotypes, the set of parameters used were same as that described by Génard *et al* (2010).

**Sugar supply**

According to a study conducted by Génard *et al*. (2003), total sugar unloading of fruit (g C per day) was deduced directly from field measurements of fruit dry mass growth. Equation 10 (Eqn 10) shows that total C supply is estimated as the sum of the carbon used for respiration and growth.

$$\frac{dC_{\square}}{dt} = \sigma_f \frac{dDW}{dt} + \frac{dC_{resp}}{dt} \quad \text{Eqn 10}$$

Here $\sigma_f$ is the carbon concentration of mesocarp (g C per gram of dry mass).

The measured sucrose to total sap sugar (sucrose + sorbitol) ratio (see ‘Measurement of sap sugar composition’ section) was used to define sap composition in terms of sucrose and sorbitol content. A unique value of sucrose sap proportion ($\lambda$ = 0.65) has been used for all genotypes. This value was assumed constant during fruit development.

Sucrose coming from sap flow can be further hydrolyzed into glucose and fructose before reaching cytosol. It has been reported that invertase activity of cell-wall decreases during fruit development in tomatoes and Rosaceae (Ranwala *et al.* 1992; Kortstee *et al.* 2007; Li *et al.* 2012; Zhang *et al.* 2014). It was assumed that sucrose fraction $\lambda_{Suc}(t)$ was not hydrolyzed by cell-wall invertase, which is a linearly increasing function of the time (day) (Eqn 11)

$$\lambda_{Suc}(t) = \frac{\lambda_{Suc} * t}{tmax} \qquad \text{Eqn 11}$$

Equation 11 shows that $t_{max}$ corresponds with maturation time (specific to the genotype), which was directly deduced from the data. In contrast the parameter $\lambda_{Suc}$ was estimated numerically. Furthermore, $\lambda_{Suc}(t)$ participates in the elaboration of flows F1 and F3 (Figure 1).

**Model selection procedure**

A model selection procedure was carried out to define model structure, following a principle of parsimony. A model without any allosteric regulation was defined first.

Following literature information, allosteric control was then tested on SDH (Archbold, 1999; Zhou *et al.*, 2006), SuSy (Schaffer & Petreikov 1997) and AI (Sampietro *et al.* 1980), and the model improvement evaluated by the Akaike information criterion (Burnham & Anderson 2002).To keep the model as simple as possible, the addition of allosteric inhibition was maintained only if a significant improvement in fitted model was observed. In the retained model, AI was inhibited by fructose and glucose. The inhibition parameter ($Ki\_{AI}$) was numerically estimated along with other parameters.

**Model parameterization**

The final model includes thirty parameters. To parameterize enzyme kinetics, $V_{max}$ was measured in a study conducted by Desnoues *et al.* (2014). In particular, given the low diversity of enzyme capacities observed across the population, an average enzyme capacity was defined per phenotypic class and year for each of the enzymes. To achieve this aim, , a polynomial curve was fitted to $V_{max}$ by means of a generalized mixed linear-effect model (Desnoues *et al.* 2014). Some $V_{max}$ values varied depending on developmental stage and/or the fructose phenotype, whereas others remained constant (Table S1). There were very small differences in $V_{max}$ between opposite fructose types but they have no significant effect on resultant sugar concentration (Desnoues *et al*. 2014).

Most $K_M$ values were fixed based on published data, which were obtained from research studies of peach or fruit (Table S1). Since different isoforms (Kanayama *et al.* 1998; Tanase & Yamaki 2000; Kanayama *et al.* 2005) were present in variable proportions, the apparent $K_M$ (depending on the proportion of each isoform) was unknown for some enzymes. Thus, apparent $K_M$ of hexokinase (HK), fructokinase (FK), and sucrose synthase (Susy) were estimated numerically.

Transport mechanisms between cytosol and vacuole were explicitly represented in this model. There is a general lack of data concerning transporters, including their number, lifetime, and evolution during cell expansion. In the absence of further information, six parameters linked to vacuolar transport kinetics were assumed to be constant and were estimated numerically (Table S1).

Overall, 14 parameters were estimated to fully calibrate the model (Table S1)

**Initialization, numerical integration and parameter estimation**

Model integration and calibration was performed using Matlab software. The ODE solver ode23s based on a modified Rosenbrock formula of order 2 (Shampine & Reichelt 1997) was used. Parameter estimation was performed using genetic algorithm (ga function, global optimization toolbox). To run simulations, initial conditions were based on concentrations of sucrose, glucose, fructose, and sorbitol. These conditions were measured for each genotype at the first stage of development. The cost function (to be minimized) was defined as the sum of squares of differences between simulated and measured fruit sugar concentrations (glucose, fructose, sorbitol, and sucrose) over an entire period of fruit development. Matlab software's ga function was used for fitting stopped when the average relative change in the best cost function value over generations was less than 1e-6. This threshold was used as the criteria of convergence in fitting process. For parameter estimation, boundary values were initially defined from literature and then increased if needed (i.e. if estimations were mostly at the boundary) to potentially offset the effect of other possible regulatory mechanisms, which were not accounted for in the model. Final estimation ranges are reported in Table S1.

To ensure good exploration of parameter space, 24 to 29 estimations were performed for each genotype by randomly varying initial population. The estimations that had not more than 10% deviation from the lowest sum of squared differences between simulations and observations for each genotype were kept for subsequent analyses. Eventually, eight estimations were kept for genotype E1, eight for genotype E22, ten for genotype E33, seven

for genotype E43, seven for genotype F106, eight for genotype F111, ten for genotype F146, ten for genotype H191, ten for genotype C216, and four for genotype C227. A PCA analysis was performed on 14 parameters' values for each of these retained estimations by using ade4 library of R software (R development Core Team 2006).

**Sensitivity Analysis**

A sensitivity analysis based on Morris method (Saltelli *et al.* 2004) was performed on cost function, which was used for parameter estimation and for identifying most influential parameters. We assumed a uniform distribution of parameters' values within estimation range. _For each of the 14 estimated parameters, the average and the variance of elementary effects (mu and sigma, respectively), as well as the mean of their absolute values (mu*) were determined by Morris method (Saltelli *et al.* 2004). A separate analysis was performed for each genotype. Matlab software was used for implementation of this model. Results are shown in Figure S10.

**Virtual classification experiment**

By randomly assigning model parameters and inputs, 100,000 virtual genotypes were simulated using Matlab software. Parameters were considered randomly by assuming a uniform distribution between minimum and maximum estimated values over the entire set of genotypes and estimations. Inputs and parameters, such as fruit weight, maturity date, initial sugar concentration, and $V_{max}$ of NI, FK and HK were considered randomly among the values used for 10 genotypes under this study. Pearson correlation between fructose-to-glucose ratio and the value of 14 model parameters were assessed using R software (R development Core Team 2006).

The same experiment was performed for another 100,000 virtual genotypes but Kfk value was fixed. For 50,000 simulations, the Kfk value was fixed at 16.58 (the average estimated value of 'standard fructose-to-glucose ratio' phenotype). For remaining 50,000 simulations, Kfk value was fixed at 1.52 (the average estimated value of 'low fructose-to-glucose ratio' phenotype). The inputs and the remaining 13 parameters were taken randomly as previously. By using "ttest" function in Matlab software, a Wilcoxon test was performed and the resultant 'fructose-to-glucose ratio' was compared at maturity.

**Acknowledgments**

We thank V. Signoret and E. Pelpoir for their help with fruit sampling, as well as Y. Gibon, P. Ballias and D. Prodhomme for their assistance at the Bordeaux Metabolome Platform at INRA Bordeaux, France. We thank C. Cheniclet for the cytological photography performed at the Bordeaux Imaging Center. We also thank B. Beauvoit, M. Dieuaide-Noubhani and Suzanne Touzeau for helpful discussions and suggestions. We are grateful to the IE-EMMAH UMR1114 team for taking care of the experimental orchard. This work was partially funded from the Agence Nationale de la Recherche, Project “Frimouss” (grant no. ANR–15–CE20–0009).

**Supporting Information**

Additional supporting information may be found in the online version of this article.

Equations S1: Model equations.

FigureS1: Evolution of the proportion of the vacuole and cytosol during peach fruit development.

Table S1: Model parameter description.

Table S2: RMSE and RRMSE between the model simulation and experimental data.

FigureS2: Evolution of the model’s flows along fruit development

FigureS3: Sucrose to sorbitol composition of phloem sap.

FigureS4: Prediction of sugars repartition between cytosol and vacuole

FigureS5: PCA of the estimated parameter values FigureS6: Boxplot of the fourteen parameter values estimated.

FigureS7: Fructose concentration with modified TpassifFru parameter value.

FigureS8: Comparison of the flows following the change of the Kfk parameter.

Table S3: Predicted variation of the cumulative flows over fruit development following the change of the KfK parameter.

FigureS9: Correlation between fructose-to-glucose ratio and model parameters via a virtual classification experiment

FigureS10: Sensitivity analysis.

**References**

**Abnasan N., Shiratake K., Yamaki S.** (1999) Change in sugar content and sorbitol - and sucrose - related enzyme activities during development of loquat (*Rriobotrya japonica* Lindl. cv. Mogi) fruit. *J. Japan. Soc. Hort. Sci*. 68(5), 942-948. DOI: 10.2503/jjshs.68.942

**Archbold DD** (1999) Carbohydrate availability modifies sorbitol dehydrogenase activity of apple fruit. *Physiol. Plant.* 105, 391-786. DOI: 10.1034/j.1399-3054.1999.105301.x

**Beauvoit BP, Colombié S, Monier A, Andrieu MH, Biais B, Bérnard C, Chéniclet C, Dieuaide-Noubhani M, Nazaret C, Mazat JP et al.** (2014) Model-assisted analysis of sugar metabolism throughout tomato fruit development reveals enzyme and carrier properties in relation to vacuole expansion. *The Plant cell* 26(8), 3224-3242. DOI: https://doi.org/10.1105/tpc.114.127761

**Biais B, Bénard C, Beauvoit B, Colombié S, Prodhomme D, Ménard G, Bernillon S, Gehl B, Gautier H, Ballias P et al.** (2014) Remarkable reproducibility of enzyme activity profiles in tomato fruits grown under contrasting environments provides a roadmap for studies of fruit metabolism. *Plant Physiol.* 164(3), 1204-1221. DOI: https://doi.org/10.1104/pp.113.231241

**Boorer K, Loo D, Frommer W, Wright E** (1996) Transport mechanism of the cloned potato H+/sucrose cotransporter StSUT1. *J. Biol. Chem.* 271(41), 25139-25144. DOI: 10.1074/jbc.271.41.25139

**Borstlap A, Schuurmans J** (2004) Sucrose transport into plasma membrane vesicles from tobacco leaves by H+ symport or counter exchange does not display a linear component. *J. Membr. Biol.* 198(1), 31-42. DOI: 10.1007/s00232-004-0657-z

**Burnham KKP, Anderson DRD** (2002) Model Selection and Multimodel Inference: A Practical Information-Theoretic Approach (2nd ed). Ecological Modelling 172

**Cantín C, Gogorcena Y, Moreno MA** (2009) Analysis of phenotypic variation of sugar profile in different peach and nectarine [*Prunus persica* (L.) Batsch] breeding progenies. *J. Sci. Food Agric.* 89, 1909-1917. DOI: 10.1002/jsfa.3672

**Chardon F, Bedu M, Calenge F, Klemens P, Spinner L, Clement G, Chietera G, Léran S, Ferrand M, Lacombe B et al.** (2013) Leaf fructose content is controlled by the vacuolar transporter SWEET17 in *Arabidopsis*. *Curr. Biol.* 23(8), 697-702. DOI: http://dx.doi.org/10.1016/j.cub.2013.03.021

**Curien G, Bastien O, Robert-Genthon M, Cornish-Bowden A, Cárdenas ML, Dumas R** (2009) Understanding the regulation of aspartate metabolism using a model based on measured kinetic parameters. *Mol. Syst. Biol.* 5(1). DOI: 10.1038/msb.2009.29.

**Desnoues E, Gibon Y, Baldazzi V, Signoret V, Génard M, Quilot-Turion B** (2014) Profiling sugar metabolism during fruit development in a peach progeny with different fructose-to-glucose ratios. *BMC Plant Biology* 14, 336. DOI: https://doi.org/10.1186/s12870-014-0336-x

**Doehlert DC** (1987) Substrate inhibition of maize endosperm sucrose synthase by fructose and its interaction with glucose inhibition. *Plant Sci.* 52, 153-157. DOI: https://doi.org/10.1016/0168-9452(87)90048-3

**Doidy J, Grace E, Kühn C, Simon-Plas F, Casieri L, Wipf D** (2012) Sugar transporters in plants and in their interactions with fungi. *Trends Plant Sci.* 17(7), 413-322. DOI: 10.1016/j.tplants.2012.03.009.

**Etienne C, Rothan C, Moing A, Plomion C, Bodénès C, Svanella-Dumas L, Cosson P, Pronier V, Monet R, Dirlewanger E** (2002) Candidate genes and QTLs for sugar and organic acid content in peach [*Prunus persica* (L.) Batsch]. *Theor. Appl. Genet.* 105, 145-304. DOI: 10.1007/s00122-001-0841-9.

**Farré EM, Tiessen A, Roessner U, Geigenberger P, Trethewey RN, Willmitzer L** (2001) Analysis of the compartmentation of glycolytic intermediates, nucleotides, sugars, organic acids, amino acids, and sugar alcohols in potato tubers using a nonaqueous fractionation method. *Plant Physiol.* 127, 685-700. DOI: https://doi.org/10.1104/pp.010280

**Fettke J, Fernie AR** (2015) Intracellular and cell-to-apoplast compartmentation of carbohydrate metabolism. *Trends Plant Sci.* 20(8),490-497. DOI: http://dx.doi.org/10.1016/j.tplants.2015.04.012

**Génard M, Bruchou C, Souty M** (1991) Variabilité de la croissance et de la qualité chez la pêche (*Prunus persica* L Batsch) et liaison entre croissance et qualité. *Agronomie* 11, 829-845

**Génard M, Souty M** (1996) Modeling the peach sugar contents in relation to fruit growth. *J. Am. Soc. Hortic. Sci.* 121(6), 1122-1131.

**Génard M, Lescourret F, Gomez L, Habib R** (2003) Changes in fruit sugar concentrations in response to assimilate supply, metabolism and dilution: a modeling approach applied to peach fruit (*Prunus persica*). *Tree Physiol.* 23(6), 373-385. DOI: 10.1093/treephys/23.6.373.

**Génard M, Bertin N, Gautier H, Lescourret F, Quilot B** (2010) Virtual profiling: a new way to analyse phenotypes. *Plant J.* 62(2), 344-355. DOI: 10.1111/j.1365-313X.2010.04152.x.

**Génard M, Baldazzi V, Gibon Y** (2014) Metabolic studies in plant organs: don't forget dilution by growth. *Front. Plant Sci.* 5: 85. DOI: 10.3389/fpls.2014.00085.

**Guo WJ, Nagy R, Chen HY, Pfrunder S, Yu YC, Santelia D, Frommer WB, Martinoia E** (2014) SWEET17, a facilitative transporter, mediates fructose transport across the tonoplast of Arabidopsis roots and leaves. *Plant Physiol*. 164(2), 777-789. DOI: 10.1104/pp.113.232751.

**Jiang F, Wang Y, Sun H, Yang L, Zhang J, Ma L** (2013) Intracellular compartmentation and membrane permeability to sugars and acids at different growth stages of peach. *Sci. Hort.* 161, 210-215. DOI: https://doi.org/10.1016/j.scienta.2013.06.037.

**Kanayama Y, Granot D, Dai N, Petreikov M, Schaffer A, Powell A, Bennett AB** (1998) Tomato fructokinases exhibit differential expression and substrate regulation. *Plant Physiol.* 117(1), 85-90. DOI: 10.1104/pp.117.1.85.

**Kanayama Y, Kogawa M, Yamaguchi M, Kanahama K** (2005) Fructose content and the activity of fructose - related enzymes in the fruit of eating - quality peach cultivars and native - type peach cultivars. *J. Japan. Soc. Hort. Sci.* 74(6), 431-436. DOI: http://doi.org/10.2503/jjshs.74.431

**King RW, Zeevaart JAD** (1974) Enhancement of phloem exudation from cut petioles by chelating agents. *Plant Physiol.* 53, 96-103. DOI: https://doi.org/10.1104/pp.53.1.96.

**Kortstee A, Appeldoorn N, Oortwijn M, Visser R** (2007) Differences in regulation of carbohydrate metabolism during early fruit development between domesticated tomato and two wild relatives. *Planta* 226(4), 929-939. DOI: 10.1007/s00425-007-0539-6.

**Li M, Feng F, Cheng L** (2012) Expression patterns of genes involved in sugar metabolism and accumulation during apple fruit development. *PLoS One* 7(3). DOI: https://doi.org/10.1371/journal.pone.0033055

**Ludewig F, Flügge UI** (2013) Role of metabolite transporters in source-sink carbon allocation. *Front. Plant Sci.* 4, 231. DOI: 10.3389/fpls.2013.00231.

**Martinoia E, Meyer S, De Angeli A, Nagy R** (2012) Vacuolar transporters in their physiological context. *Annu. Rev. Plant Biol.* 63, 183-213. DOI: 10.1146/annurev-arplant-042811-105608.

**Morell M, Copeland L** (1985) Sucrose synthase of soybean nodules. *Plant Physiol.* 78, 149-154. DOI: https://doi.org/10.1104/pp.78.1.149.

**Moriguchi T, Yamaki S** (1988) Purification and characterization of sucrose synthase from peach (*Prunus persica*) fruit. *Plant Cell Physiol.* 29(8), 1361-1366. DOI: https://doi.org/10.1093/oxfordjournals.pcp.a077647

**Moriguchi T, Ishizawa Y, Sanada, T** (1990) Differences in sugar composition in *Prunus persica* fruit and classification by the principal component analysis. *J. Japan. Soc. Hort. Sci.* 59(2), 307-312. DOI: http://doi.org/10.2503/jjshs.59.307.

**Moriguchi R, Sanada T, Yamaki S** (1991) Properties of acid invertase purified from peach fruits. *Phytochemistry* 30(1), 95-97. DOI: https://doi.org/10.1016/0031-9422(91)84105-2

**Nadwodnik J, Lohaus G** (2008) Subcellular concentrations of sugar alcohols and sugars in relation to phloem translocation in *Plantago major*, *Plantago maritima*, *Prunus persica*, and *Apium graveolens*. *Planta* 227(5), 1079-1089. DOI: 10.1007/s00425-007-0682-0.

**Nägele T, Henkel S, Hörmiller I, Sauter T, Sawodny O, Ederer M, Heyer A** (2010) Mathematical modeling of the central carbohydrate metabolism in Arabidopsis reveals a substantial regulatory influence of vacuolar invertase on whole plant carbon metabolism. *Plant Physiol.* 153(1), 260-272. DOI: 10.1104/pp.110.154443.

**Nägele T, Weckwerth W** (2014) Mathematical modeling reveals that metabolic feedback regulation of SnRK1 and hexokinase is sufficient to control sugar homeostasis from energy depletion to full recovery. *Front. Plant Sci.* 5, 365. DOI: 10.3389/fpls.2014.00365.

**Oura Y, Yamada K, Shiratake K, Yamaki S** (2000) Purification and characterization of a NAD(+)-dependent sorbitol dehydrogenase from Japanese pear fruit. *Phytochemistry* 54(6), 567-572. DOI: https://doi.org/10.1016/S0031-9422(00)00158-8.

**Pangborn RM** (1963) Relative taste intensities of selected sugars and organic acids. *J. Food Sci.* 28, 726-733. DOI: 10.1111/j.1365-2621.1963.tb01680.x.

**Patrick JW, Botha FC, Birch RG** (2013) Metabolic engineering of sugars and simple sugar derivatives in plants. *Plant Biotech. J.* 11(2), 142-156. DOI: 10.1111/pbi.12002.

**Preisser J, Komor E** (1991) Sucrose uptake into vacuoles of sugarcane suspension cells. *Planta* 186. DOI: 10.1007/BF00201505.

**Quilot B, Génard M, Kervella J, Lescourret F** (2004a) Analysis of genotypic variation in fruit flesh total sugar content via an ecophysiological model applied to peach. *Theor. Appl. Genet.* 109, 440-449. DOI: 10.1007/s00122-004-1651-7

**Quilot B, Wu B, Kervella J, Génard M, Foulongne M, Moreau K** (2004b) QTL analysis of quality traits in an advanced backcross between Prunus persica cultivars and the wild relative species P. davidiana. *Theor. Appl. Genet.* 109(4), 884-897. DOI: 10.1007/s00122-004-1703-z.

**Quilot B, Kervella J, Génard M, Lescourret F** (2005) Analysing the genetic control of peach fruit quality through an ecophysiological model combined with a QTL approach. *J. Exp. Bot.* 56(422), 3083-3092. DOI: 10.1093/jxb/eri305.

**Quilot-Turion, B, Génard, M, Valsesia, P, and Memmah, M-M** (2016) Optimization of Allelic Combinations Controlling Parameters of a Peach Quality Model. *Front. Plant Sci.* 7,1873. DOI: 10.3389/fpls.2016.01873.

**R Development Core Team** (2006) R: A language and environment for statistical computing, R Foundation for Statistical Computing, Vienna, Austria

**Ranwala AP, Suematsu C, Masuda H** (1992) Soluble and wall-bound invertases in strawberry fruit. *Plant Sci.* 84(1), 59-64. DOI: https://doi.org/10.1016/0168-9452(92)90208-4.

**Reymond M, Muller B, Tardieu F** (2004) Dealing with the genotype×environment interaction via a modelling approach: a comparison of QTLs of maize leaf length or width with QTLs of model parameters. *J. Exp. Bot*. 55(407), 2461-2472. DOI: 10.1093/jxb/erh200

**Rios-Estepa R, Lange B** (2007) Experimental and mathematical approaches to modeling plant metabolic networks. *Phytochemistry* 68(16-18), 2351-2374. DOI: 10.1016/j.phytochem.2007.04.021

**Rohwer J, Botha F** (2001) Analysis of sucrose accumulation in the sugar cane culm on the basis of in vitro kinetic data. *Bioch. J.* 358(Pt 2), 437-445.

**Ross HA, Davies HV** (1992) Purification and characterization of sucrose synthase from the cotyledons of *Vicia faba* L. *Plant Physiol.* 100, 1008-1013.

**Sampietro AR, Vattuone MA, Prado FE** (1980) A regulatory invertase from sugar cane leaf-sheaths. *Phytochemistry* 19, 1637-1642. DOI: https://doi.org/10.1016/S0031-9422(00)83784-X

**Saltelli, A, Tarantola, S, Campolongo, F, Ratto, M** (2004) Sensitivity Analysis in Practice - A Guide to Assessing Scientific Models. Wiley

**Schaffer AA, Petreikov M** (1997) Inhibition of fructokinase and sucrose synthase by cytosolic levels of fructose in young tomato fruit undergoing transient starch synthesis. *Physiol. Plant.* 101(4), 800-806. DOI: 10.1111/j.1399-3054.1997.tb01066.x

**Shampine L, Reichelt M** (1997) The MATLAB ODE Suite. *SIAM J. Sci. Comput.* 18(1), 1-22. DOI: https://doi.org/10.1137/S1064827594276424

**Sheveleva EV, Marquez S, Chmara W, Zegeer A, Jensen RG, Bohnert HJ** (1998) Sorbitol-6-phosphate dehydrogenase expression in transgenic tobacco: high amounts of sorbitol lead to necrotic lesions. *Plant Physiol*. 117(3), 831-839.

**Shiratake K, Kanayama Y, Yamaki S** (1997) Characterization of hexose transporter for facilitated diffusion of the tonoplast vesicles from pear fruit. *Plant Cell Physiol*. 38

**Sun Z, Li Y, Zhou J, Zhu SH** (2011) Effects of exogenous nitric oxide on contents of soluble sugars and related enzyme activities in 'Feicheng' peach fruit. *J. Sci. Food Agric*. 91, 1795-2595. DOI: 10.1002/jsfa.4384.

**Sweetlove LJ, Fernie AR.** (2013) The Spatial Organization of Metabolism Within the Plant Cell. *Annu. Rev. Plant Biol.* 64, 723-746. DOI: 10.1146/annurev-arplant-050312-120233.

**Tanase K, Yamaki S** (2000) Sucrose synthase isozymes related to sucrose accumulation during fruit development of japanese pear (*Pyrus pyrifolia* Nakai). *J. Japan. Soc. Hort. Sci.* 69(6), 671-676. DOI: http://doi.org/10.2503/jjshs.69.671

**Uys L, Botha F, Hofmeyr JHS, Rohwer J** (2007) Kinetic model of sucrose accumulation in maturing sugarcane culm tissue. *Phytochemistry* 68, 2375-2392. DOI: https://doi.org/10.1016/j.phytochem.2007.04.023

**Voster DJ, Botha F** (1998) Partial purification and characterisation of sugarcane neutral invertase. *Phytochemistry* 49(3), 651-655. DOI: https://doi.org/10.1016/S0031-9422(98)00204-0

**Wei X, Liu F, Chen C, Ma F, Li M** (2014) The *Malus domestica* sugar transporter gene family: identifications based on genome and expression profiling related to the accumulation of fruit sugars. *Front. Plant Sci.* 5, 569. DOI: 10.3389/fpls.2014.00569.

**Wu B, Quilot B, Génard M, Li S, Zhao J, Yang J, Wang Y** (2012) Application of a SUGAR model to analyse sugar accumulation in peach cultivars that differ in glucose–fructose ratio. *J. Agric. Sci.* 150, 53-63. DOI: https://doi.org/10.1017/S0021859611000438

**Yamaki S, Moriguchi T** (1989) Seasonal fluctuation of sorbitol-related enzymes and invertase activities accompanying maturation of japanese pear (*Pyrus serotina* Rehder var. culta Rehder) fruit. *J. Japan. Soc. Hort. Sci.* 57(4), 602-607. DOI: http://doi.org/10.2503/jjshs.57.602

**Yamaki S, Ino M** (1992) Alteration of cellular compartmentation and membrane permeability to sugars in immature and mature apple fruit. *J. Am. Soc. Hortic. Sci.* 117(6), 951-954.

**Zhang HP, Wu JY, Qin GH, Yao GF, Qi KJ, Wang LF, Zhang SL** (2014) The role of sucrose-metabolizing enzymes in pear fruit that differ in sucrose accumulation. *Acta Physiol. Planta.* 36, 71-77.

**Zhou R, Cheng L, Dandekar A** (2006) Down-regulation of sorbitol dehydrogenase and up-regulation of sucrose synthase in shoot tips of the transgenic apple trees with decreased sorbitol synthesis. *J. Exp. Bot.* 57:3647-365. DOI: 10.1093/jxb/erl112

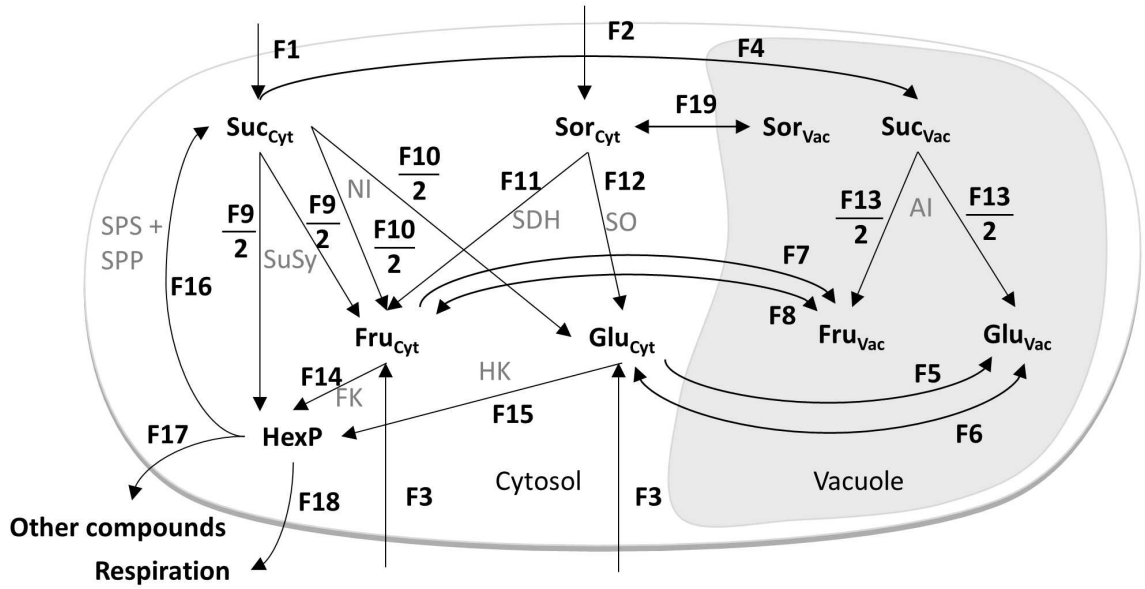


**Figure 1.** Schematic network of peach fruit sugar accumulation model. Arrows represent carbon flows. The corresponding kinetic equations are reported in the Supplemental Information file (Equations S1). Abbreviations are as follows: Suc, sucrose; Sor, sorbitol; Fru, fructose; Glu, glucose; HexP, hexose-phosphate; cyt, cytosol; Vac, vacuole; SuSy, sucrose synthase; NI, neutral invertase; SDH, sorbitol dehydrogenase; SO, sorbitol oxidase; AI, acid invertase; SPS, sucrose phosphate synthase; SPP, sucrose-phosphate phosphatase; FK, fructokinase; HK, hexokinase.

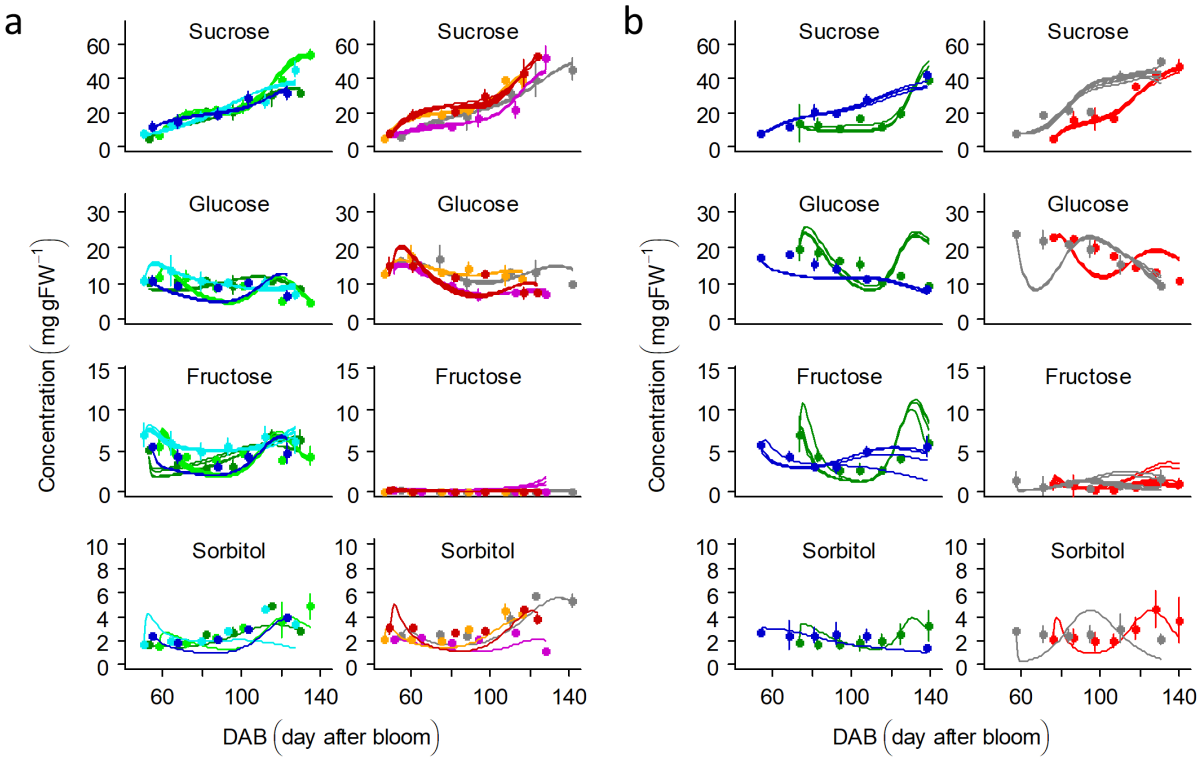


**Figure 2.** Evolution of the concentration (mg $gFW^{-1}$) of sugars within the fruit during development (DAB, days after bloom). A comparison of model simulations (lines) with experimental data (circles represent the mean and segments represent standard deviation). Only simulations with no more than 10% deviation from the lowest sum of squared differences between simulations and observations were presented. Eight genotypes are presented on panel a) four genotypes had a 'standard fructose-to-glucose ratio' (left) and four genotypes had a 'low fructose-to-glucose ratio' phenotype (right). Panel b) presents two different genotypes: one with a 'standard fructose-to-glucose ratio' phenotype (left) and another with a 'low fructose-to-glucose ratio' phenotype (right) in two years, namely, 2010 (green and red) and 2011 (blue and grey).

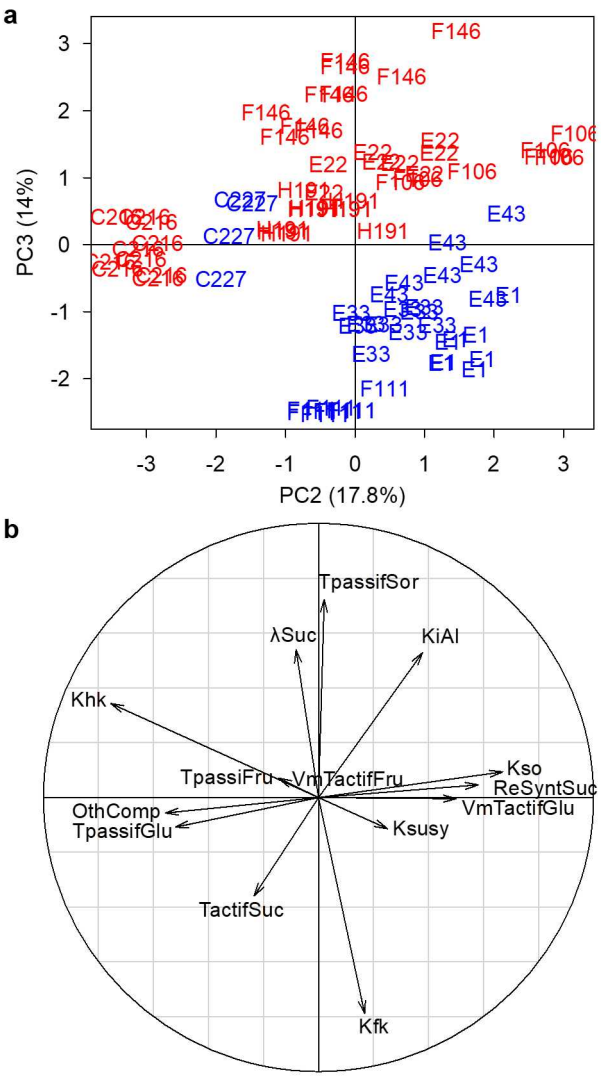


**Figure 3.** PCA of the 14 parameter values estimated for the five genotypes with the 'standard fructose-to-glucose' phenotype (blue) and five genotypes with 'low fructose-to-glucose' phenotype (red). a) Projection of different simulations for each genotype with components 2 and 3. b) Correlation of variables with components 2 and 3.

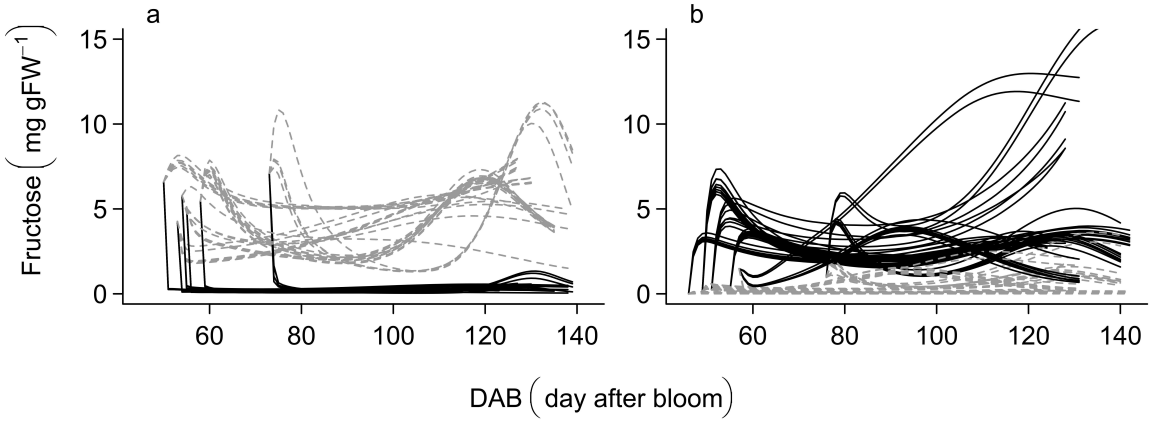


**Figure 4.** Fructose concentration (mg g FW$^{-1}$) during fruit development (DAB, days after bloom). (a) Black lines correspond to simulations of five genotypes with 'standard fructose-to-glucose ratio' phenotypes; average values of Kfk parameter estimated from genotypes with 'low fructose-to-glucose ratio' phenotype; (b) simulations of the five genotypes with 'low fructose-to-glucose ratio' phenotype with average values of Kfk parameters estimated from genotypes with 'standard fructose-to-glucose ratio' phenotype. Grey dotted lines correspond with original fructose concentration simulations.

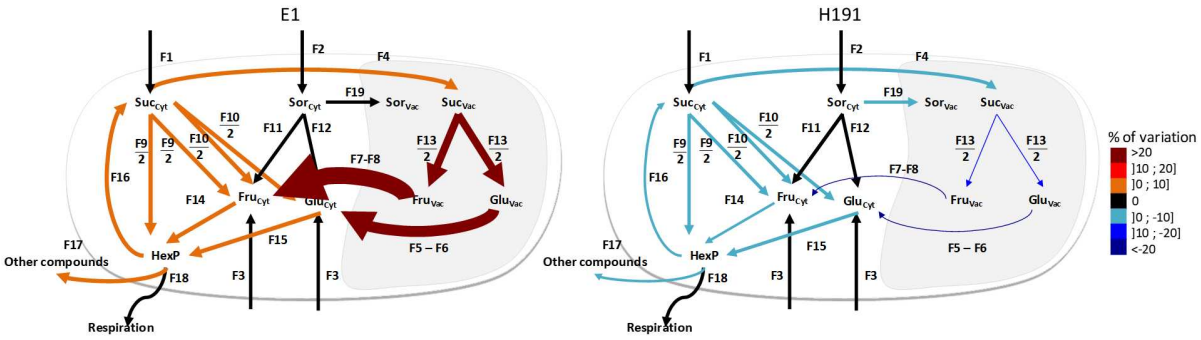


**Figure 5.** Predicted cumulative flow of distribution was assessed according to changes in KfK parameter. For each metabolic flow, the integral over fruit development was calculated and compared with the corresponding value without Kfk modification. Arrow size and color are proportional to the percentage of variation between modified and normal cumulative flow. The flows F1, F2, and F3 were not modified; their size correspond to the ratio of 1. Large and

red arrows denote that modified KfK parameter induces an increase of flow. Smaller and blue arrows denote that modified KfK parameter induces an increase of flow. *Left*: Flux map of a genotype with ‘standard-fructose-to-glucose’ phenotype (E1). The values of KfK parameter was replaced by average value of KfK parameter, which was estimated for five genotypes with ‘low fructose-to-glucose’ phenotype. *Right*: Flux map of a genotype with ‘low fructose-to-glucose’ phenotype (H191). The value of KfK parameter was replaced by the average value of KfK parameter, which was estimated for five genotypes with ‘standard-fructose-to-glucose’ phenotype. Maps corresponding to all genotypes are presented in Figure S8.

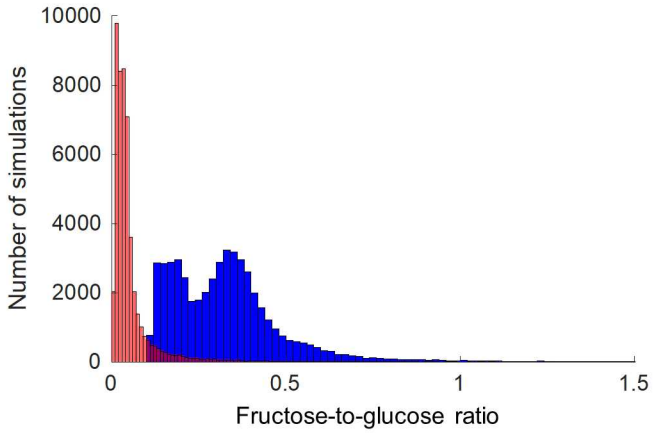


**Figure 6.** Fructose-to-glucose ratio at maturity for 100,000 simulations for which parameters were estimated and fruit weight was taken randomly except that Kfk value was fixed at the average estimated value of ‘standard fructose-to-glucose ratio’ phenotype for 50,000 simulations (blue) and at average estimated value of ‘low fructose-to-glucose ratio’ phenotype for 50,000 other simulations (red).

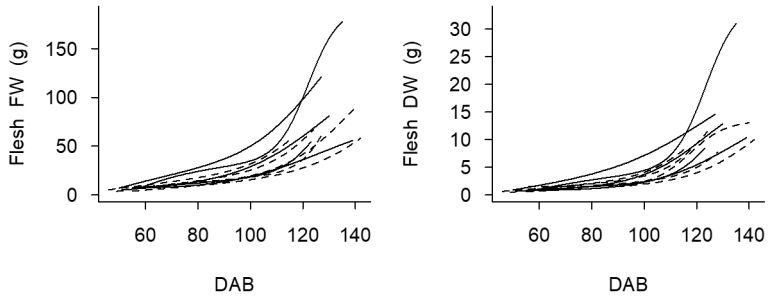


**Figure 7.** Time (DAB, days after bloom) courses of flesh fresh weight (FW) and dry weight (DW) for ten genotypes. Five genotypes with the ‘standard fructose-to-glucose ratio’ phenotype are represented with continuous lines, and five genotypes with a ‘low fructose-to-glucose ratio’ phenotype are represented with dashed lines.